

Temperature, moisture and mode-mixity effects on copper leadframe/EMC interfacial fracture toughness

Hai T. Tran · M. Hossein Shirangi ·
Xiaolu Pang · Alex A. Volinsky

Received: 3 March 2013 / Accepted: 8 November 2013 / Published online: 21 November 2013
© Springer Science+Business Media Dordrecht 2013

Abstract A systematic investigation and characterization of the interfacial fracture toughness of the bi-material copper leadframe/epoxy molding compound is presented. Experiments and finite element simulations were used to investigate delamination and interfacial fracture toughness of the bi-material. Two dimensional simulations using virtual crack closure technique, virtual crack extension and J-integral proved to be computationally cheap and accurate to investigate and characterize the interfacial fracture toughness of bi-material structures. The effects of temperature, moisture diffusion and mode-mixity on the interfacial fracture toughness of the bi-material were considered. Testing temperature and moisture exposure significantly reduce the interfacial fracture toughness, and should be avoided if possible.

Keywords Energy release rate · Interfacial fracture toughness · Copper leadframe · Epoxy molding compound · Delamination · Finite element simulation

1 Introduction

Many modern systems consist of at least two materials, and the interface is defined as a boundary between two dissimilar materials. In most cases, the interface is the weakest point, and the system reliability is largely affected by the mechanical behaviour of the interface. Microelectronic packages and assemblies typically consist of multiple layers of materials with dissimilar physical properties. Stresses induced by mechanical and/or thermal loading can initiate and propagate interfacial delamination, especially near the free edges. Such interfacial delamination can lead to the multilayered microelectronic package failure.

Among bi-material systems used in microelectronic packages, copper leadframe and epoxy molding compound (EMC) is an important combination. EMCs are used for protecting the semiconductor chips from the external environment, specifically from external physical forces, impact and pressure, chemical forces, moisture, heat, ultraviolet rays, while electrically insulating the semiconductor devices (Komori and Sakamoto 2009). Figure 1 shows the cross-section of a microelectronic package with copper leadframe/EMC.

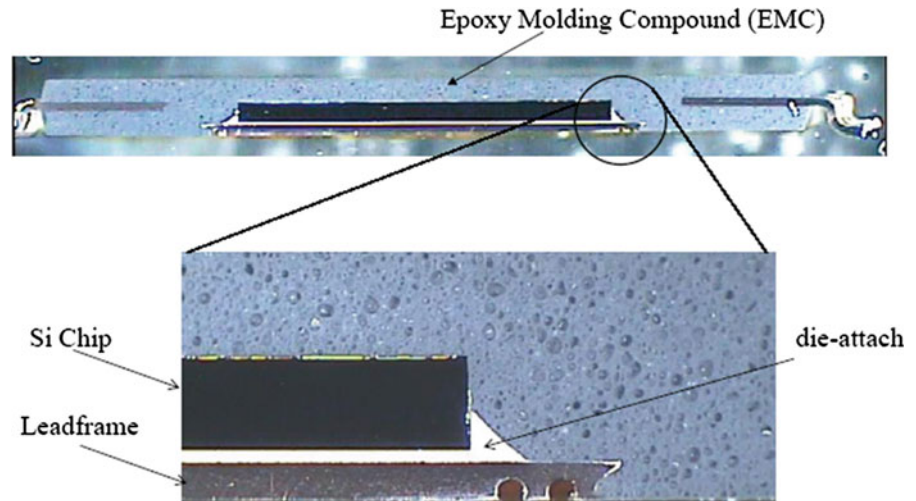
There have been several studies addressing adhesion between copper and EMC. Wong et al. (2006) used

H. T. Tran · A. A. Volinsky (✉)
Department of Mechanical Engineering,
University of South Florida,
4202 E. Fowler Ave ENB118, Tampa, FL 33627, USA
e-mail: volinsky@eng.usf.edu; volinsky@usf.edu

M. H. Shirangi
Robert Bosch GmbH, Automotive Electronics,
70442 Stuttgart, Germany

X. Pang
Department of Materials Physics and Chemistry,
University of Science and Technology Beijing,
Beijing 100083, China

Fig. 1 Cross-section of a microelectronic package with copper leadframe/EMC



an atomic force microscope to characterize nanoscale adhesion forces in the Cu/SAM/EMC system. Fan et al. (2005) used a series of button shear tests along with the finite element method (FEM) to evaluate the interfacial adhesion between the EMC and copper. Xie and Sitaraman (2003) performed standard tensile tests for determining the interfacial fracture toughness of copper/epoxy, while monitoring the crack length. They also performed fatigue tests to study interfacial delamination, followed by fatigue crack propagation. Chan and Yuen (2009) used Fourier transform infrared multiple internal reflection technique to detect moisture at the epoxy/copper interface.

In this work, based on experiments and numerical simulations, a fast, simple and comprehensive methodology is proposed to investigate the interfacial delamination propagation and characterize the fracture toughness of the interface between copper leadframe and EMC. In Fracture Mechanics' energy criterion approach, the crack propagates when the strain energy release rate (SERR) G , which is the driving force for the crack propagation, is equal to its critical value G_c , known as the interfacial fracture toughness. The values of G_c were calculated by the finite element (FE) simulations in this paper. Temperature, moisture and mode-mixity effects on the leadframe/EMC adhesion (i.e. interfacial fracture toughness) were investigated.

Although analytical expressions for the total SERR are available for some simple interfacial crack problems (Hutchinson and Suo 1992), they involve considerable mathematical complexity. For complicated geometries, or loading conditions, analytical expres-

sions may be unavailable and need to be solved numerically. Fortunately, the total SERR can be obtained using FE-based techniques, such as virtual crack closure technique (VCCT), virtual crack extension technique (VCE), J-integral. In comparison with other FEM-based methods, VCCT has many advantages. First, G can be easily computed by VCCT in conjunction with the FE analysis, since VCCT does not make any assumptions for the form of the stresses and displacements. Therefore, singularity elements are not required at the crack tip. Second, the physical meaning of VCCT is clear: energy to create new surfaces. It combines both force and displacement opening. Third, in contrast to VCE, in VCCT, the second analysis is not required. This leads to a faster calculation. Fourth, the mode-mixity of the fracture can be obtained by VCCT, since it gives individual mode components of SERR. The mode-mixity can also be obtained by the J-integral, but not as convenient as VCCT, especially with the FE software Ansys. Last, VCCT does not require a special mesh arrangement around the crack front. It is not mesh sensitive, and even a coarse mesh can work. However, the major limitation of the VCCT is that it can only be applied to linear elastic fracture (to be discussed later). With these advantages, this work focuses on the VCCT and uses other methods as references.

2 Simulations

In this study, three FEM-based methods were implemented with the commercial general purpose FE

software package, Ansys, to calculate SERRs of fractures. The three methods include VCCT (the main focus), VCE, and the J-integral. In order to get the most accurate result of the SERRs, the convergence analysis was used to find the optimal mesh.

2.1 Virtual crack closure technique: VCCT

VCCT for SERR calculation was originally proposed in 1977 by Rybicki and Kanninen, based on Irwin’s crack closure integral (Irwin 1957). Although the VCCT has a significant advantage over other methods, it has not yet been implemented into most of the large commercial general-purpose FE codes.

With the definition of SERR as $G = -\frac{\partial \Pi}{\partial A}$, where A is the crack area and Π is the potential energy of the system supplied by internal strain energy and external forces, the mode I and mode II components of the SERR, G_I and G_{II} are calculated for the four-node elements (similarly for other advanced cases, such as eight-node elements), as shown in Fig. 2 (Krueger 2002):

$$G_I = -\frac{1}{2\Delta a} \cdot Z_i \cdot (w_l - w_{l^*}) \tag{1}$$

$$G_{II} = -\frac{1}{2\Delta a} \cdot X_i \cdot (u_l - u_{l^*}) \tag{2}$$

where a is the length of the elements at the crack front, X_i and Z_i are the forces at the crack tip (nodal point i). The relative displacements behind the crack tip are calculated from the nodal displacements at the upper crack

face u_l and w_l (nodal point l), and the nodal displacements u_{l^*} and w_{l^*} at the lower crack face (nodal point l^*), respectively. The crack surface ΔA created is calculated as $\Delta A = \Delta a \cdot l$, where it is assumed that the two dimensional model is of unit thickness, l . The total SERR G is calculated from the individual mode components as:

$$G = G_I + G_{II} + G_{III} \tag{3}$$

where $G_{III} = 0$ for the two dimensional case.

2.2 Virtual crack extension method: VCE

In the VCE method, which was implemented in Ansys, two analyses are performed, one with the crack length a , and the other with the crack length $a + \Delta a$. If the potential energy Π (strain energy) for both cases is stored, the SERR can be calculated from:

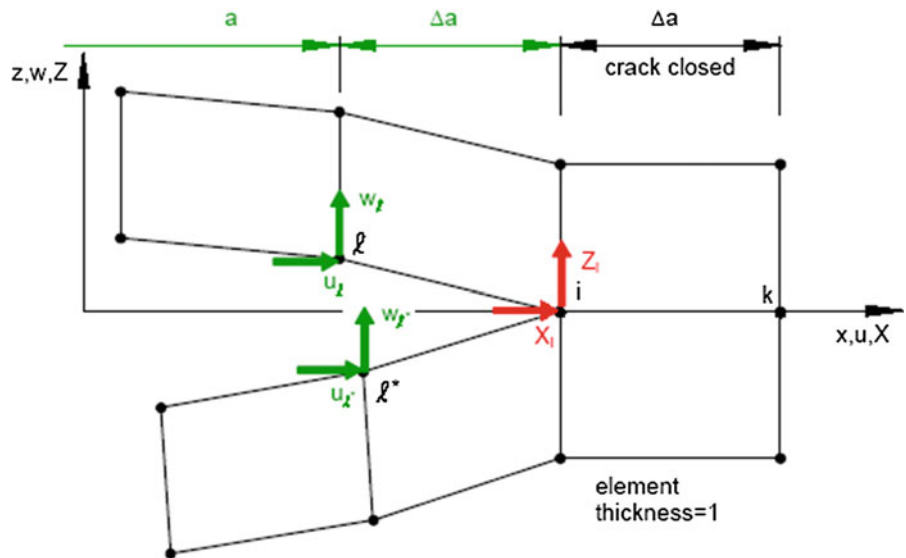
$$G = -\frac{\Delta \Pi}{\Delta A} = -\frac{\Pi_{a+\Delta a} - \Pi_a}{B \Delta a} \tag{4}$$

where B is the thickness of the fracture model.

2.3 The J-integral method

J-integral was first introduced by Rice and Sih (1968), due to the difficulties involved in computing the stresses close to the crack in nonlinear elastic or elastic-plastic materials. It can be shown (Anderson 2005) that if a monotonic loading is assumed (without any plastic

Fig. 2 VCCT for the four-node elements (Krueger 2002)



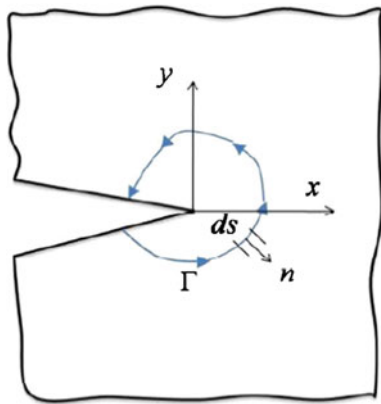


Fig. 3 Definition of the J-integral path

unloading), the J-integral can be used to compute the energy release rate of plastic materials for small scale deformations. In its simplest form, the J-integral can be defined as a path-independent line integral that measures the strength of the singular stresses and strains near the crack tip (Fig. 3). For a nonlinear elastic body containing a crack, the J integral is defined as:

$$J = \int_{\Gamma} w dy - T_i \frac{\partial u_i}{\partial x} ds \quad (5)$$

where $w = \int_0^{\varepsilon_{ij}} \sigma_{ij} d\varepsilon_{ij}$ is the strain energy density, $T_i = \sigma_{ij} n_j$ is the traction vector, Γ is an arbitrary contour around the tip of the crack, n is the unit vector normal to Γ , and σ , ε , u are the stress, strain, and displacement fields, respectively.

J-integral has been implemented in Ansys, version 11 and latter versions in four steps, where the J-integral is calculated at the solution phase of the analysis, after a sub-step has converged, and then Ansys stores the values in the results file.

3 Experiments

3.1 Samples and equipment

The samples were made from copper leadframe and EMC. Various raw material ingredients were added to the EMC in order to meet the requirements of reliability, physical properties and moldability. The typical ingredients were phenolic resins, epoxy resins, fused silica as filler, coupling agents, curing promoter, and a release agent, all of which influence the adhesion

Table 1 Composition of the EMC

EMC components	Parameters
Epoxy resin	Multi aromatic + Biphenyl
Hardener	Low water absorption
Flame retardant system	No FR
Filler content	88/80 weight/volume, %
Filler shape	All spherical (average 50 μm diameter)
Spiral flow	1,143 mm
Gelation time (175 °C)	30 s
Flexural modulus	2,450 kgf/mm ²
Flexural strength	15 kgf/mm ²

Table 2 Composition of the copper leadframe

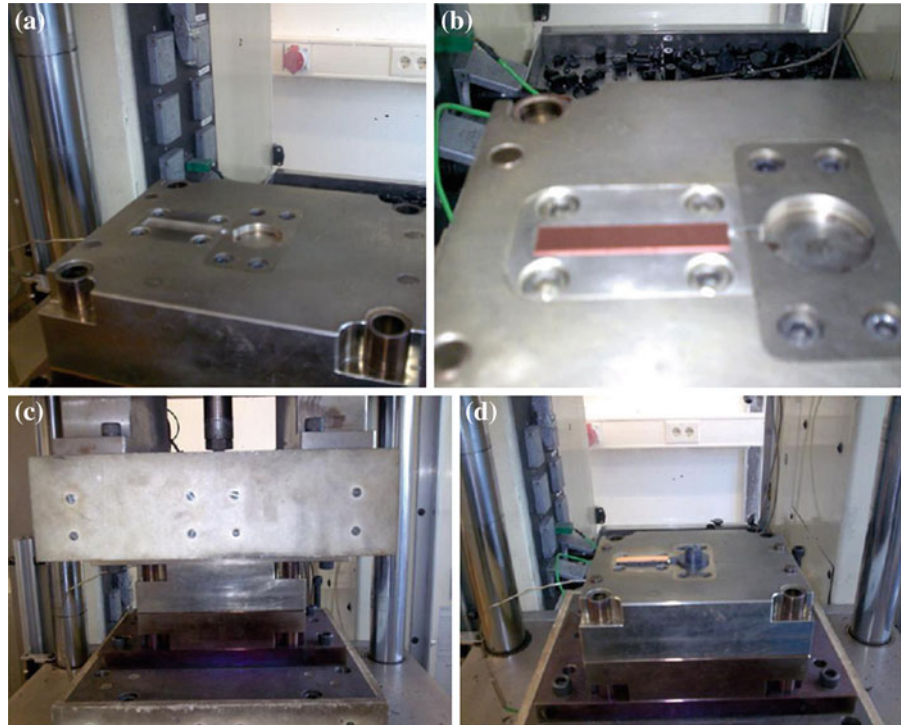
Cu	Fe	P	Pb	Zn
Balance	2.1–2.6 wt%	0.015 wt%	0.03 wt%	0.05–0.2 wt%

strength and moldability of the resulting product. These raw materials were mixed and kneaded under heat into a homogeneous mixture in a kneader or a roll mixer. Generally, the materials were cooled, while kneaded into a sheet, and then pulverized. The powdery material was pelletized into pellets, which were used in the transfer molding step. Commercial EMC pellets were provided by the vendors and kept in the refrigerator at freezing temperature (below -10°C) to avoid undesired chemical changes, or contamination. The composition of the EMC investigated in this study is shown in Table 1.

A leadframe is a thin layer of metal that connects the wiring from tiny electrical terminals on the semiconductor surface to the large-scale circuitry in electrical devices and circuit boards. The leadframe used in this study is a copper-based alloy with the chemical composition listed in Table 2. The surface of the copper leadframe sheet was uniformly covered by Nickel-Palladium-Gold (NiPdAu).

Transfer molding is normally the preferred method for encapsulating or packaging a semiconductor chip with an EMC. It is generally a fast, consistent manufacturing technique that results in high-quality parts. This relatively simple process can be simply automated, which makes it suitable for a lean manufacturing line (Komori and Sakamoto 2009). The transfer molding process used for the bi-material samples was similar to

Fig. 4 Transfer molding for fabricating Cu/EMC samples. **a** Mold form. **b** Leadframe placed in the mold form. **c** Injection of EMC. **d** Release of the molded sample from the mold form



that of the plastic encapsulated microcircuits, including the following steps:

- (1) Set the leadframe (substrate) connected to the semiconductor chip (here only the leadframe plate) into the cavities of a heated mold (Fig. 4b).
- (2) Set the molding compound tablet into the pot of the molding machine.
- (3) Close the mold die tightly and melt the molding compound under 170–180 °C mold temperature, and pour it into the mold under pressure (Fig. 4c).
- (4) After applying pressure for 45–90 s, when the molding compound has been fully cured, open the mold and release the molded parts. This completes the encapsulation process.

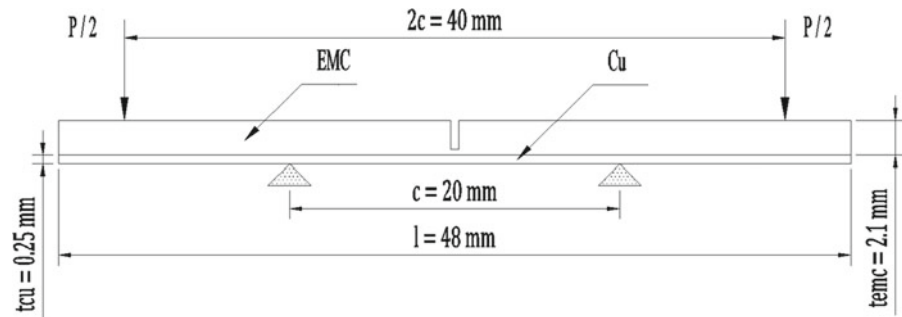
To fabricate the bi-material samples, leadframe plates were machined into $48 \times 10 \times 0.4 \text{ mm}^3$ strips and molded. After the transfer molding, the samples were placed in an environmental chamber for the post-mold curing at 175 °C for 6 h to complete the polymerization process of the EMC.

In order to get the interfacial fracture toughness of the bi-material samples, a highly precise testing device is required. A computer-controlled Instron 5848 micro-tester was used for this purpose (Fig. 5).



Fig. 5 Instron 5848 micro-tester

Fig. 6 4PB delamination test set-up



3.2 Four-point bending delamination test

The critical forces, which were achieved from the four-point bending (4PB) experiments, were used to obtain the critical SERRs G_c (i.e. interfacial fracture toughness) of the interface between copper leadframe and EMC. They were determined by the FEM simulations using the three mentioned methods: VCCT, VCE and J-integral. The verification of simulations was performed using an analytical solution (Eq. 7). Based on the critical SERRs obtained from different specimens tested at different temperatures, the temperature dependence of the interfacial fracture toughness was investigated.

The upper EMC layer of the sample was notched with a diamond blade to get the depth of the notch, approximately 80% of the EMC thickness. Figure 6 shows the 4PB test setup, and Fig. 7 shows the sample before and after the test. The distance between the two loading pins was fixed at $c = 20$ mm, and the distance between the two supports was fixed at $2c = 40$ mm.

A major issue in fracture mechanics simulations is the large degree of freedom of the FE model. It is well known that a three dimensional FE model becomes very computationally expensive to implement, even with the minimal number of elements across the thicknesses, which in turn causes a very large aspect ratio in the simulation model. This work presents an effort to develop a simpler, low-cost two dimensional model to evaluate the system. With the test conformation, the problem can be assumed to be plane strain. The very good agreement between FE analysis results and the analytical solution confirmed this assumption (discussed in Sect. 4.1, Fig. 11).

In this problem, the LEFM was assumed to hold true. First, the reaction forces and applied displace-

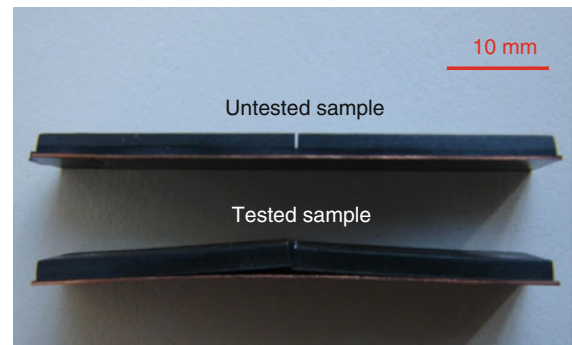


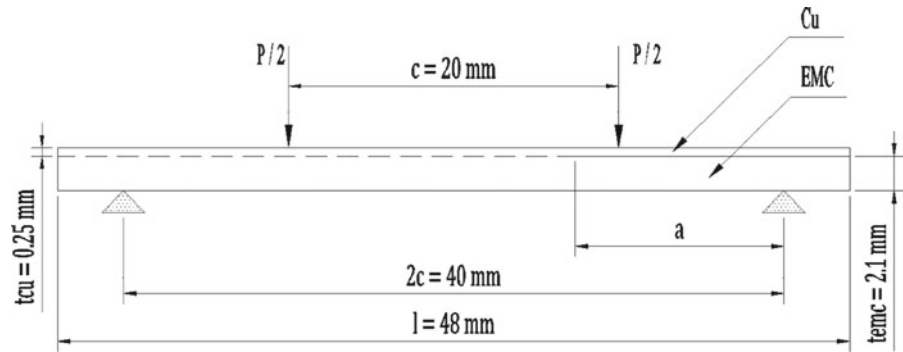
Fig. 7 4PB delamination specimen before and after the test

ment, up to the delamination point, were always linear. Second, there is no significant plastic deformation at the moment. In other words, the plastic zone was much smaller than the stress intensity factor dominated field. Volinsky et al. (1999) proposed the relationship between the energy release rate and the plastic zone size as the following:

$$G \approx c \frac{\sigma_{ys}^2}{E} \left(\ln \left[\frac{c}{b} \right] - 1 \right) \quad (6)$$

where c is the plastic zone size, b is Burgers vector, E is the Young's modulus, σ_{ys} is the yield stress of, in this case, the copper layer. With the value of $G = 17.78 \text{ J/m}^2$ (25 °C test temperature, 1 mm/min loading rate), we estimated the plastic zone size to be $5.52 \times 10^{-3} \text{ mm}$, which is much smaller than the Cu layer thickness of 0.25 mm. Last, the 4PB tests were performed at a relatively high displacement rate of 1 mm/min, and crack propagation happened within a couple of seconds after starting the test, and took normally less than one second until the crack reached the supports. Therefore, the visco-elastic effects due to the stress relaxation within such a short crack propagation time were found to be almost negligible. For the above

Fig. 8 4ENF set-up



reasons the LEFM can be applied for these tests and the visco-elastic deformation of the EMC layer can be neglected.

The SERR of 4PB delamination test exhibits steady-state characteristics when the interfacial crack reaches a minimum length, and does not exceed the distance between the inner supports (in this case, $c = 20$ mm). This value of G_c , is the difference between the strain energy in the un-cracked and cracked beams. Applying the beam theory and assuming LEFM, G can be calculated as in (Charalambides et al. 1989):

$$G = \frac{M^2(1 - \nu_{Cu}^2)}{2E_{Cu}} \left(\frac{1}{I_{Cu}} - \frac{\lambda}{I_c} \right) \tag{7}$$

where $\lambda = [E_{Cu}(1 - \nu_{EMC}^2)]/[E_{EMC}(1 - \nu_{Cu}^2)]$, $M = PL/2b$. I_c and I_{Cu} are the moments of inertia of the composite beam and Cu, respectively, which can be calculated as:

$$I_c = \frac{t_{EMC}^3}{12} + \frac{\lambda t_{Cu}^3}{12} + \frac{\lambda t_{EMC} t_{Cu} (t_{EMC} + t_{Cu})^2}{4(t_{EMC} + \lambda t_{Cu})} \quad \text{and} \quad I_{Cu} = \frac{t_{Cu}^3}{12}$$

In Eq. (7), the initial cracks are symmetric, and both cracks propagate simultaneously at the same load. The equation provides the interfacial fracture toughness, G_c , when the load, P , is substituted with the critical fracture load, P_c .

3.3 Four-point bending end-notched flexure test

In order to propose a comprehensive methodology for interfacial fracture toughness characterization, this section focuses on the mode II fracture. Since the interfacial fracture toughness is strongly mode-dependent,

the four-point bending end-notched flexure (4ENF) test was used instead of the 4PB. Another reason of choosing 4ENF test is that in comparison with the conventional three-point bending end-notched flexure test, the 4ENF test has a more stable crack growth, making it, in this work, a better tool to analyze the effects of moisture on the interfacial fracture toughness of bi-materials.

Figure 8 shows the test set-up of the 4ENF for the determination of the resistance to delamination (critical SERR, or interfacial fracture toughness). Until now, there is no acceptable analytical formula for the 4ENF specimens, made of two different materials. For that reason, the interfacial fracture toughness for the 4ENF delamination tests was obtained through numerical computation using FE-based techniques. Similar to the 4PB, LEFM was assumed to hold true for the 4ENF with the loading rate of 1 mm/min. In FEM simulations, VCCT was used, since it can give the SERR for each individual fracture mode.

4 Calculations and results

4.1 Interfacial fracture toughness of the four-point bending specimen

The 4PB delamination test can be performed in one, or two steps, including pre-cracking. Here, the single step approach was used, in which the whole fracture test is performed in a single step, without pre-cracking. In (Shirangi et al. 2008), it was shown that the critical forces are almost the same either with, or without pre-cracking.

To verify the FE model, samples were loaded monotonically under displacement-controlled rate of 1.0 mm/min at room temperature. Figure 9 shows a typical load-displacement curve of the 4PB fracture

Fig. 9 The force—displacement curve of a 4PB delamination test at room temperature

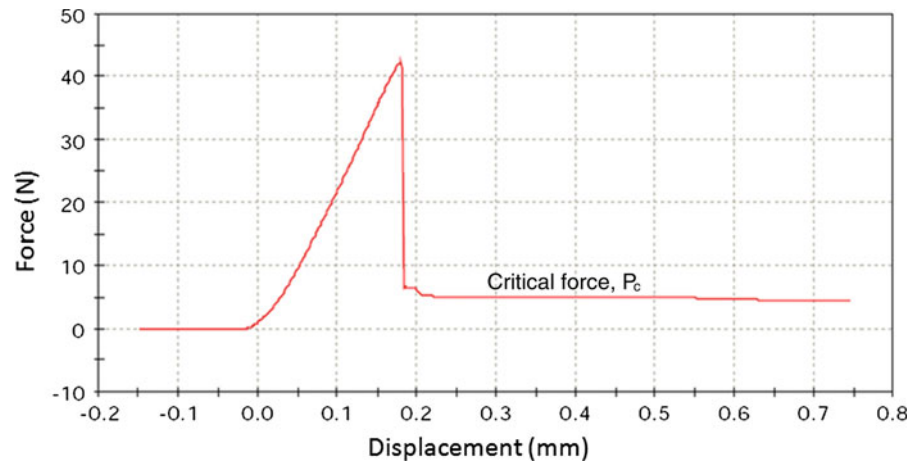
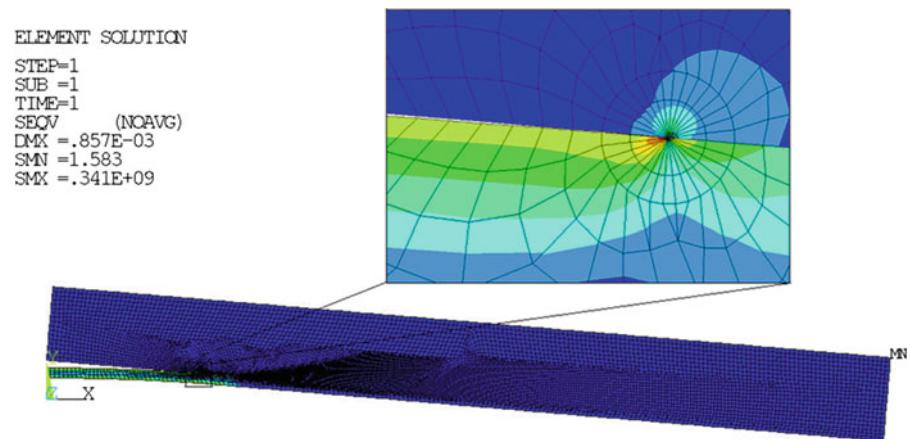


Fig. 10 Deformation shape of the 4PB model with optimal mesh, using singularity elements at the crack tip



test. The slope of the linear part of the curve corresponds to the stiffness of the whole structure. The peak force represents the required force for fracture of the upper layer (EMC) through the notch, and does not provide any information about the interface fracture toughness. The vertical part of the curve shows that the notch has been broken down, and the interface has been reached. Afterwards, the crack advanced along the interface. This constant force during crack propagation represents the critical force required to propagate the crack. Its constant value suggests that the critical SERR using 4PB fracture test does not depend on the crack length.

As mentioned above, three FE approaches, implemented in Ansys, were used to calculate the critical SERRs of the 4PB specimens' fracture. In order to find the most accurate result for G_c , the convergence analysis was used to find the optimal mesh. The comparison

between the approaches and the analytical solution was also performed.

The simulation model of the test is shown in Fig. 10. Taking advantage of the symmetry, only half of the 4PB specimen is modelled. To prevent rigid body translation, the x-displacement of the points, where the two loads $P/2$ are applied, is fixed. The analysis was performed in plane strain. The optimal mesh was obtained by performing the convergence analysis, in which three mesh parameters involved are the radius of the first row elements at the crack tip, the number of elements in the circumferential direction and the maximum element size. The two types of meshing—using *singularity elements at the crack tip* and using *mesh refinement around the crack tip*, were implemented. There was not much difference between the two mesh types with respect to the obtained G_c values. Moreover, the computational time in the latter type is three times longer than the

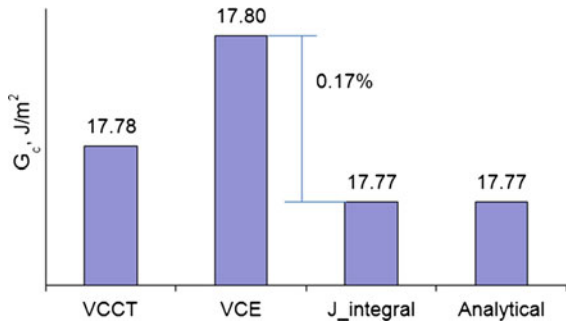


Fig. 11 Critical SERRs calculated by the four methods

first one. Therefore, the former type was chosen. The mechanical properties of the bi-material, obtained by uniaxial tensile tests, are: $E = 135$ GPa and $\nu = 0.34$ for copper leadframe, and $E = 30$ GPa and $\nu = 0.24$ for EMC at room temperature.

Figure 11 shows the results of G (J/m²) calculated by the four methods: VCCT, VCE, J-integral, and the analytical solution of Eq. (7), under the average critical load P_c (average of 5 tests) of 5.56 N (25 °C test temperature, 1.0 mm/min loading rate). These SERRs are at the average mode-mixity of 15.46°. It can be seen that G_c values calculated with the four methods are nearly the same. With a very good agreement with the other methods, and with the capability of finding the components of G , corresponding to the mode I and mode II separately (thus the capability of finding the mode-mixity), VCCT was chosen as the main method and the others were used for reference.

4.2 Temperature effect on the interfacial fracture toughness

Temperature dependence of the interfacial fracture toughness of the copper leadframe/EMC interface was investigated. After keeping all the 4PB samples for 6 h in a heat chamber at 175 °C to complete the polymerization process of the EMC, they were tested at various temperatures of 25, 85, 130, 175, 210, and 250 °C (5 samples for each test temperature). The samples were loaded monotonically under displacement-controlled rate of 1.0 mm/min. Since the Young’s modulus of EMC is temperature dependent, it was determined using uniaxial tensile tests at various temperatures (Table 3), identical to the fracture experiments temperatures.

Table 3 Young’s modulus of EMC at varying temperature

Temperature (°C)	Young’s modulus of EMC (GPa)
25	30
85	25
130	2
175	2
210	1
250	1

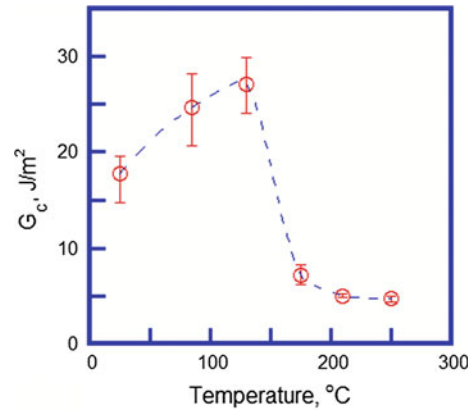


Fig. 12 G_c calculated by VCCT using experimental critical force at different temperatures

When testing at elevated temperatures and time scales, where visco-elastic deformation may affect the interfacial fracture toughness, LEFM is believed to be still valid, since the load-displacement curves are all linear, up to the point of delamination propagation. In this case, any significant visco-elastic deformation that may occur in a sample is assumed to occur on a very local scale at the crack tip region as a part of the crack growth process. Moreover, the EMC used in this work is cross-linked, which means, according to Swallowe (1999), that the viscoelasticity effects can be neglected.

Figure 12 shows the fracture toughness of the copper leadframe/EMC interface, which was calculated by VCCT, as a function of the test temperature. The results from 5 samples, along with the average value at each temperature, are shown (17.78 J/m² at 25 °C, 23.99 J/m² at 85 °C, 27.80 J/m² at 130 °C, 7.21 J/m² at 175 °C, 5.02 J/m² at 210 °C, and 4.71 J/m² at 250 °C). G_c was also calculated by using other approaches (i.e. VCE, J-integral and analytical formula) for comparison, and all of them give nearly the same values.

It can be seen that after an initial increase at the early stages of the temperature rise, the interfacial fracture toughness significantly decreases with the test temperature. The glass transition temperature of the EMC is about 130 °C. Therefore, the interfacial fracture toughness undergoes a significant change around the glass transition temperature.

4.3 Interfacial fracture toughness of the four-point bending end-notched flexure specimen

The same samples were used, but after molding, they were kept for 6 h in the heat chamber at 175 °C to complete the EMC polymerization process. Moreover, instead of notching the upper layer (EMC), in the 4ENF samples, the pre-crack at the interface was made by a sharp steel blade. The testing machine was Instron 5848 micro-tester. The distance between the two loading pins was fixed at 40 mm, and the distance between the two supports was fixed at 20 mm. Samples were loaded monotonically under displacement-controlled rate of 1.0 mm/min at room temperature.

Figure 13 shows the force—displacement curve of the 4ENF test. The slope of the linear part of the curve (A-B) corresponds to the stiffness of the whole structure. The force at point B represents the required force (critical force) for the interfacial delamination. This force was used to determine the interfacial fracture toughness, G_c , in the simulation. From point B to C the crack propagates, until it stops at point C. Afterwards, the load increases linearly again, and the slope represents the stiffness of the EMC only.

In order to find the most accurate result of the SERR, the convergence analysis was also used to find the

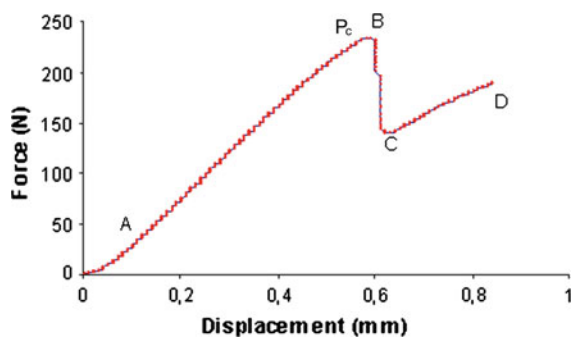


Fig. 13 The force—displacement graph of the 4ENF delamination test at room temperature

optimal mesh in the same manner as for the 4PB specimens. The VCCT was applied to obtain the critical SERR for the 4ENF specimens. In this simulation, contact elements and target elements are required at the pre-crack surface to prevent elements penetration. Besides, the geometry non-linearity was also considered to obtain a better result. As mentioned in the 4PB case, two types of meshing, which are *using singularity elements at the crack tip* and *using mesh refinement around the crack tip*, were used, and the former type was proven to be better.

Components of the critical SERR, G_{Ic} , G_{IIc} , and the total critical SERR, G_c , were obtained by VCCT (Fig. 14), based on the pre-crack lengths and the critical forces from 5 tests. Under the average critical load, P_c , of 229.9 N and the average pre-crack length of 11.72 mm, G_{Ic} , G_{IIc} and G_c of 3.64 J/m², 196.31 J/m² and 198.16 J/m², were obtained, respectively. This SERR value corresponds with the average mode-mixity angle of 82.27°.

4.4 Moisture effect on the interfacial fracture toughness

The effect of moisture on the interfacial fracture toughness of copper leadframe/EMC was investigated. All the fracture tests were performed at room temperature and the loading rate of 1.0 mm/min. Before the tests, except for the samples tested in dry condition, all the other ones were placed into a moisture chamber for 1, 2, 3, 4 and 5 weeks (5 samples for each category) at 85 °C and 85 % relative humidity. Only the EMC layer absorbs moisture. An electronic balance scale was used for weighing the samples to calculate the amount of moisture absorbed by the EMC layer. The weight gain of the samples at the time of testing can be determined as:

$$\text{weight gain (\%)} = \frac{M_t - M_0}{M_0} \times 100 \% \quad (8)$$

where M_t is the weight of the sample at time t (in weeks) and M_0 is the dry weight before the moisture preconditioning. Figure 15 shows the average mass of the moisture absorbed with respect to time. It can be recognized that the moisture absorption reached saturation at around 4 weeks at the weight gain of 0.22 %.

From Fig. 16, which shows the critical SERRs of the moisture preconditioned samples, calculated by VCCT, based on experimental critical forces, the effect of

Fig. 14 Deformation shape of the 4ENF model with optimal mesh using singularity elements at the crack tip

```

ELEMENT SOLUTION
STEP=1
SUB =8
TIME=1
SEQV      (NOAVG)
DMX =.403
SMN =.169E-04
SMX =835.289
    
```

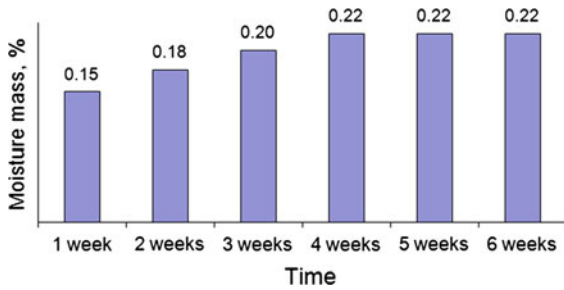
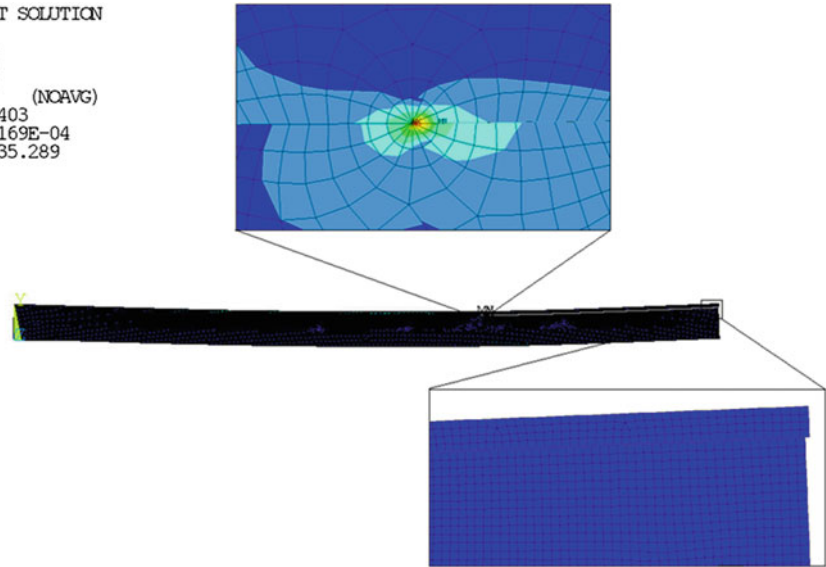


Fig. 15 The average moisture mass absorbed by EMC

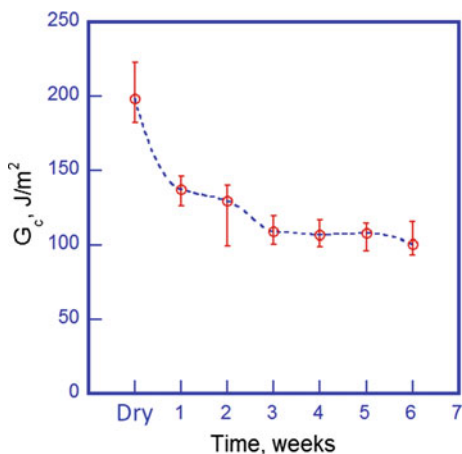


Fig. 16 G_c calculated by VCCT using experimental critical forces of the moisture absorbed specimens

moisture diffusion in humid chamber on the interfacial fracture toughness of bi-materials Cu lead-frame/EMC can be seen. The initial interfacial fracture toughness of 198.16 J/m² in dry condition reduced significantly to 137.1 J/m² after one week of moisture absorption, and then continued to decrease slightly with moisture exposure time. Finally, the interfacial fracture toughness hardly changed when the moisture absorption of the specimens was around 20% (108.89 J/m² at 3 weeks, 106.59 J/m² at 4 weeks, 107.53 J/m² at 5 weeks and 100.43 J/m² at 6 weeks).

The effect of moisture on the interfacial fracture toughness is strong enough to prevent the interface from humid environment in service. However, once exposed, the moisture effect is minimal after a certain time of around three weeks at 85 °C and 85 % relative humidity. Interfacial fracture toughness decreases by a factor of two in 6 weeks of moisture exposure, compared with the dry conditions.

4.5 Mode-mixity effect on the interfacial fracture toughness

The effect of mode-mixity ψ (also called mode angle, or phase angle), which is defined as $\tan^2 \psi = \frac{G_{II}}{G_I}$, on the interfacial fracture toughness has been widely investigated. For example, [Liechti and Chai \(1991\)](#)

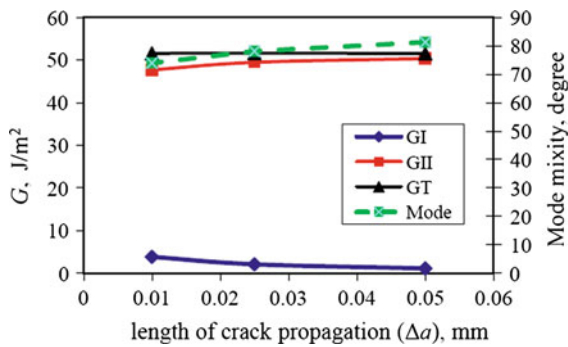


Fig. 17 The mode-mixity for a Cu/EMC interface calculated by VCCT varies only 5° when the element size is reduced to one fifth of the initial size (Shirangi 2010)

proposed a method to find the range of in-plane fracture mode-mixity and contact zone that can be obtained from bi-material samples. In that work, the crack opening displacement was measured and the values obtained with FE solutions were matched to get the mixed mode fracture parameters. Agrawal and Karlsson (2006) have shown a method to obtain mode-mixity for a bimaterial interface crack using VCCT with the 4PB model. Moreover, as discussed in (Shirangi 2010), it was concluded that if the element size is small enough to get a convergence of the total G value, the shift of the mode-mixity due to the element size is almost equal for all problems, provided that the same element size is used (Fig. 17). In other words, the mode-mixity values resulted from VCCT are consistent, even with an existing shift, whether positive or negative, in the calculated mode-mixity. This section extends the Agrawal's work by using 4PB tests together with 4ENF tests to characterize the effect of mode-mixity on the interfacial fracture toughness of copper lead-frame/EMC.

Figure 18 shows the critical SERR G_c , calculated for the two test geometries (4PB and 4ENF) of the lead-frame/EMC, as a function of the phase angle. From the 4PB delamination test at room temperature and the loading rate of 1.0 mm/min, a mean fracture toughness of 17.78 J/m² was obtained. The average interfacial fracture toughness found in the 4ENF test for the same conditions was much higher, at 198.16 J/m². This phenomenon can be explained by the mode-mixity angle. Interfacial fracture toughness strongly depends on the mode-mixity, as it increases with the contribution of the mode II fracture. In the 4PB delamination test, the average phase angle is 15.46°, which means that the fracture is close to the mode I. In the 4ENF test, the

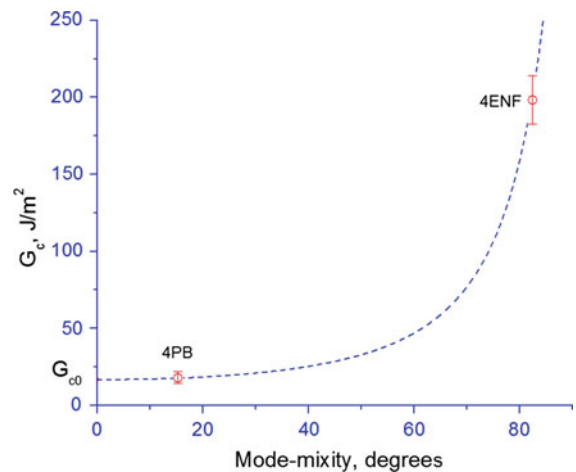


Fig. 18 Interfacial fracture toughness as a function of the phase angle for the 4PB and 4ENF tests, along with the empirical fit of Eq. (10)

average phase angle is 82.27°, which means that the fracture is mostly mode II.

Several relationships have been proposed to characterize interfacial fracture toughness as a function of the phase angle (Hutchinson and Suo 1992). There are results in the literature, both experimental and theoretical, that exhibit similar behaviour, such as (Liechti and Chai 1992) and (Jensen and Thouless 1993). The most realistic description of the functional dependence of the interfacial toughness on the mode-mixity was proposed by Hutchinson and Suo (1992):

$$G_c = G_{c0}[1 + \tan^2(\psi(1 - \lambda))] \quad (9)$$

where G_{c0} is the mode I interfacial toughness with respect to $\psi = 0$ and λ is an adjustable parameter. By fitting the results of this work, the interfacial fracture toughness and the mode-mixity relationship for the bi-materials copper lead-frame/EMC was achieved (Fig. 18). In this case $G_{c0} = 16.78$ J/m² and $\lambda = 0.111$, yielding the following G_c phase angle dependence:

$$G_c = 16.78[1 + \tan^2(0.889\psi)] \quad (10)$$

5 Summary

Two dimensional simulations with the methods, such as the Virtual Crack Closure Technique, the Virtual Crack Extension and the J-integral have been proven accurate and computationally cheap to find the SERR

and together with the critical force obtained experimentally, the interfacial fracture toughness of a bi-material structure was calculated.

This work is a systematic investigation and characterization of the interfacial fracture toughness of the bi-material copper lead-frame/EMC. The temperature dependence of the interfacial fracture toughness, the moisture diffusion effect on the fracture toughness and the relationship between the fracture toughness and the mode-mixity have been investigated.

The results of this work can be generally applied to predict the delamination, as well as to characterize the interfacial fracture toughness between the two layers of dissimilar materials under different environmental conditions.

References

- Agrawal A, Karlsson AM (2006) Obtaining mode mixity for a bimaterial interface crack using the virtual crack closure technique. *Int J Fract* 141:75–98
- Anderson TL (2005) *Fracture mechanics-fundamentals and applications*. CRC Press, Boca Raton, FL
- Chan EKL, Yuen MMF (2009) Study of interfacial moisture diffusion at epoxy/Cu interface. *J Adhesion Sci Technol* 23:1253–1269
- Charalambides PG, Lund J, Evans AG, McMeeking RM (1989) A test specimen for determining the fracture resistance of bimaterial interface. *J Appl Mech* 111:77–82
- Fan HB, Chung PWK, Yuen MMF, Chan PCH (2005) An energy-based failure criterion for delamination initiation in electronic packaging. *J Adhesion Sci Technol* 19:1375–1386
- Hutchinson JW, Suo Z (1992) Mixed mode cracking in layered materials. *Adv Appl Mech* 29:63–191
- Irwin GR (1957) Analysis of stresses and strains near the end of a crack traversing a plate. *J Appl Mech* 24:361–364
- Jensen HM, Thouless MD (1993) Effects of residual stresses in the blister test. *Int J Solids Struct* 30:779–795
- Komori S, Sakamoto Y (2009) Development trend of epoxy molding compound for encapsulating semiconductor chips. In: *Materials for advanced packaging*. Springer, New York, pp 339–363
- Krueger R (2002) *The virtual crack closure technique: history, approach and applications*. ICASE, Hampton, VA
- Liechti KM, Chai YS (1991) Biaxial loading experiments for determining interfacial fracture toughness. *Trans ASME* 58:680–687
- Liechti KM, Chai YS (1992) Asymmetric shielding in interfacial. Fracture under in-plane shear. *J Appl Mech* 59:295
- Rice JR, Sih GC (1968) Plane problems of cracks in dissimilar media. *J Appl Mech* 32:418–423
- Shirangi MH, Gollhardt A, Fischer A, Müller WH, Michel B (2008) Investigation of fracture toughness and displacement fields of copper/polymer interface using image correlation technique. In: *Proceedings of the 41st international symposium on microelectronics (IMAPS2008)*, Providence, USA
- Shirangi HM (2010) *Simulation-based Investigation of interface delamination in plastic IC packages under temperature and moisture loading*. PhD thesis, Fraunhofer Institute IZM, Berlin, Germany
- Swallowe GM (1999) *Mechanical properties and testing of polymers*. Springer Science and Business Media Dordrecht
- Volinsky AA, Tymiak NI, Kriese MD, Gerberich WW, Hutchinson JW (1999) Quantitative modeling and measurement of copper thin film adhesion. *Mat Res Soc Symp Proc* 539:277–290
- Wong CKY, Gu H, Xu B, Yuen MMF (2006) A new approach in measuring Cu-EMC adhesion strength by AFM. *IEEE Trans Compon Packag Technol* 29(3):543–550
- Xie W, Sitaraman SK (2003) Investigation of interfacial delamination of a copper-epoxy interface under monotonic and cyclic loading: experimental characterization. *IEEE Trans Compon Packag Technol* 26(4):447–452